

Dynamic grit chamber modelling: dealing with particle settling velocity distributions

Queralt Plana , Paul Lessard  and Peter A. Vanrolleghem 

ABSTRACT

Grit chambers are meant to reduce the impact of inorganic particles on equipment and processes downstream. Despite their important role, characterization and modelling studies of these process units are scarce, leading to a lack of knowledge and suboptimal operation. Thus, this study presents the first dynamic model, based on mass balances and particle settling velocity distributions, for use in a water resource recovery facility (WRRF) simulator for design and optimization of grit removal units.

Key words | grit particle characteristics, settling process, wastewater quality modelling

Queralt Plana  (corresponding author)
Peter A. Vanrolleghem 
modelEAU,
Université Laval,
1065, Avenue de la Médecine, Québec, QC G1 V
0A6,
Canada
E-mail: queralt.plana.1@ulaval.ca

Paul Lessard 
Département de génie civil et de génie des eaux,
Université Laval,
1065, Avenue de la Médecine, Québec, QC G1 V
0A6,
Canada

Queralt Plana
Paul Lessard
Peter A. Vanrolleghem
CentrEau, the Québec Water Research Center,
Université Laval,
1065, Avenue de la Médecine, Québec, QC G1 V
0A6,
Canada

INTRODUCTION

Grit chambers can be found at the headworks of most water resource recovery facilities (WRRFs) to protect the equipment and processes downstream and maintain the performance of primary and secondary treatments (WEF 2016). Despite their important role, characterization and modelling studies of these process units are scarce because they have always been considered to have a low influence on secondary treatment and studies often start from primary effluent. Importantly, grit removal efficiency is increasingly questioned by utilities since grit is still found to accumulate in downstream processes (McNamara *et al.* 2009). In addition, only a low percentage of particles found in wastewater are grit particles, i.e. 5–10% (w/w), which makes them difficult to measure under typical sampling and analysis situations (Qasim 1999; WEF 2016).

The characteristics of particulate pollutants at the inlet, outlet and underflow of grit chambers are rarely documented (Rife & Botero 2012). This lack of knowledge leads to an improper grit definition, a non-existing standard protocol for sampling and characterization, and a non-existing standard protocol for evaluating the removal performance of

grit chambers (WEF 2016). Moreover, modelling has been limited to very simple static models for percentage removal of total suspended solids (TSS) or complex hydrodynamic models focusing on flow patterns (i.e. computational fluid dynamic (CFD) models) (WEF 2016).

Since a grit chamber is a sedimentation process, the particles' separation efficiency depends on the gravitational force, wastewater particle settling characteristics and hydraulic behaviour (WEF 2016). Thus, regarding the heterogeneity of the particles into wastewater, the goal of this study is to properly characterize the influent in view of grit chamber modelling and to propose a new dynamic model based on the particle settling velocity distribution (PSVD) approach. Models based on this PSVD approach have already been presented for other settling units adjacent to grit chambers, such as primary clarifiers (Bachis *et al.* 2015), combined sewer retention tanks (Maruéjols *et al.* 2012), stormwater tanks (Vallet *et al.* 2014) and sewer systems (Ledergerber *et al.* 2019), and which have been considered as a source of inspiration to model grit chambers.

MATERIALS AND METHODS

In this study, full-scale grit chambers of a combined sewage WRRF in the Québec City area (Canada) were evaluated. The WRRF has a capacity of 36,000 people equivalent and an average design flow of 18,760 m³/d. The system studied consists of two 35 m³ vortex grit chambers with an upper part with a diameter of 4.2 m and 1.88 m height and a lower part with a diameter of 1.5 m and 2 m height (Figure 1). They have a maximum capacity of 50,940 m³/d each. With the current operating conditions, the hydraulic retention time varies between one and four minutes.

First, to characterize the particles around the grit chamber, the ViCAs (French acronym for settling velocity in wastewater) protocol (Chebbo & Gromaire 2009) was used. However, the standard 0.7 m-ViCAs column had to be upgraded to a 2 m column to better estimate the high settling velocities of the particles of interest (Plana *et al.*

2018). Several samples were collected at different flow and TSS conditions to evaluate how the PSVD varies.

To study the solids dynamics around the grit chamber, RSM-30 automated monitoring stations (Primodal, Hamilton, ON, Canada) were installed to collect long-term continuous on-line data at high frequency. The stations were equipped with several sensors to measure TSS at inlet and outlet (Plana 2020). In addition, to ensure the quality of the data series, a rigorous maintenance protocol was applied together with state-of-the-art data management and treatment (Alferes *et al.* 2013).

To build the hydraulic model of the grit chamber, two tracer tests at different flow conditions were performed. The tests consisted of a pulse input with the Rhodamine WT fluorescent dye. This tracer was chosen because it has no influence on the hydraulic behaviour of the tank (i.e. the same transport characteristics as water, no modification of the water density, no reactions with nor absorption onto solids, highly soluble and not toxic) (Gujer 2008). After

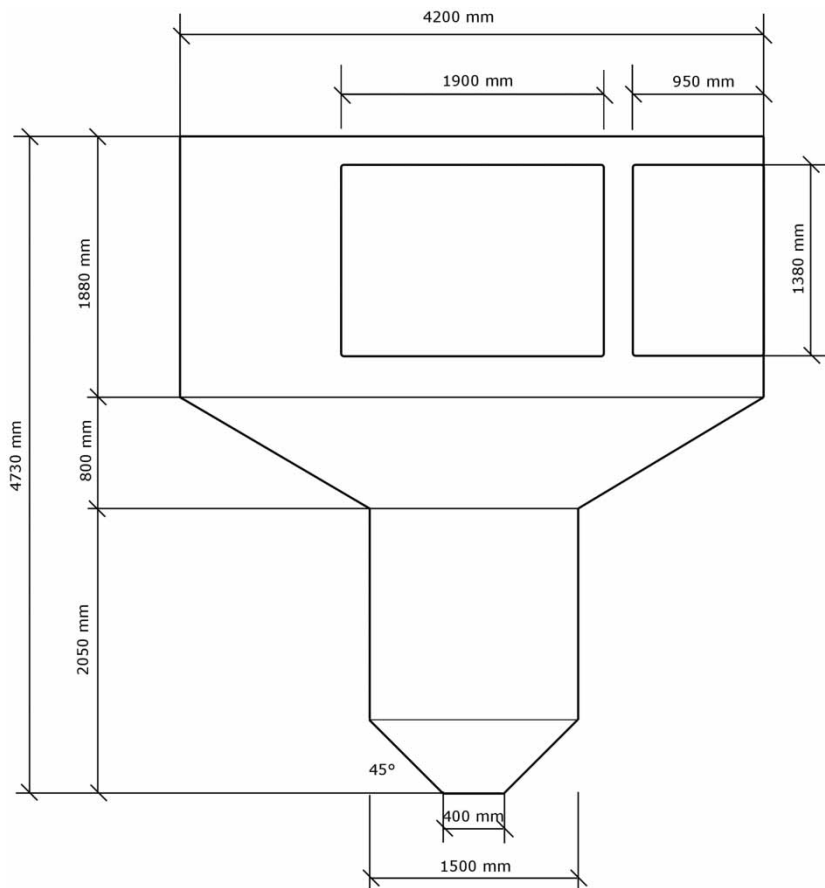


Figure 1 | Profile of the vortex grit chamber at the Saint-Nicolas WRRF. The inlet channel is the square next to the wall, and the outlet channel is the square in the middle of the upper part of the grit chamber.

tracer injection, samples were collected at the outlet of the grit chamber and fluorometric analyses were performed to study the system response.

Then, the PSVD model, based on mass balances and particle settling velocity distributions, was developed to reproduce the TSS dynamics at the outlet and underflow of the grit chamber. It consists of the fractionation of the TSS in a determined number of particle classes, each class being characterized by a mean settling velocity extracted from the experimental PSVD curves (see Figure 2) (Bachis et al. 2015; Maruėjouls et al. 2015).

The 1-D layered model was implemented in the modelling and simulation software WEST (mikebydhi.com), dividing the tank in a limited number of homogeneous layers to represent the vertical TSS profile. For example, in Figure 3, the hydraulic diagram of the PSVD model for primary clarifiers is presented (Bachis et al. 2015). The tank is fed through the fifth layer with a flow Q_{in} . The flow at the outlet (Q_{out}) is modelled out of the first layer while the underflow ($Q_{underflow}$) is modelled as the outlet of the tenth layer. Between layers, and depending on the location of the feed layer, there may be flows going up or down: Q_{up} is the flow transported to layers above, Q_{down} is the flow transported to layers below (Bachis et al. 2015). Also, a particle flux is observed between layers of the tank; $J_{up}^*(i)$ and $J_{down}^*(i)$ are the mass of particulate pollutant transported up and down (depending on the layer), hence the ‘*’ to indicate its optional presence above or below the feeding layer

by advection, and $J_{settling}$ is the mass of particulate pollutant settling from the layer above. Then, for each layer i with a height H_{layer} , a dynamic mass balance is constructed for the individual particle class n to predict the evolution of its concentration (C_n) (Tik et al. 2014; Bachis et al. 2015):

$$\frac{dC_n(i)}{dt} = \frac{1}{H_{layer}} (J_{up,n}^*(i+1) - J_{up,n}^*(i) + J_{down,n}^*(i-1) - J_{down,n}^*(i) + J_{settling,n}(i-1) - J_{settling,n}(i)) \quad (1)$$

In contrast to the PSVD model proposed for primary clarifiers by Bachis et al. (2015), a mixing flow between layers was added to better represent the induced vortex forces in the grit chamber. This was inspired by the work of Vallet et al. (2014) (see Figure 3). The mass balance, now also including the mixing fluxes (J_{mix}) for layer i and particle class n , becomes:

$$\frac{dC_n(i)}{dt} = \frac{1}{H_{layer}} (J_{up,n}^*(i+1) - J_{up,n}^*(i) + J_{down,n}^*(i-1) - J_{down,n}^*(i) + J_{settling,n}(i-1) - J_{settling,n}(i) + J_{mix,n}(i+1) + J_{mix,n}(i-1) - 2 \times J_{mix,n}(i)) \quad (2)$$

where the J_{mix} is calculated as follows:

$$J_{mix,n}(i+1) = \frac{Q_{mix}}{A} \times C_n(i) \quad (3)$$

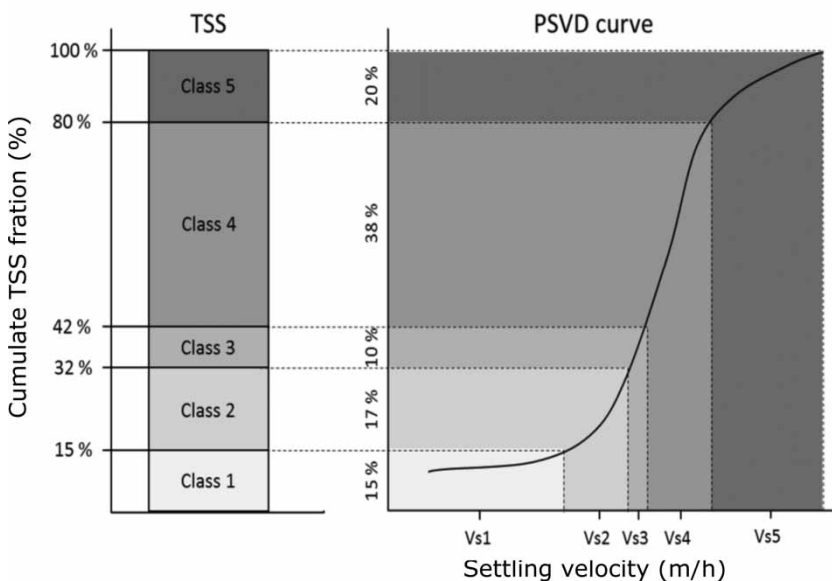


Figure 2 | Concept of TSS fractionation from a measured PSVD curve needed to calibrate the PSVD model, in this case with five classes each with their settling velocity V_s (Maruėjouls et al. 2015).

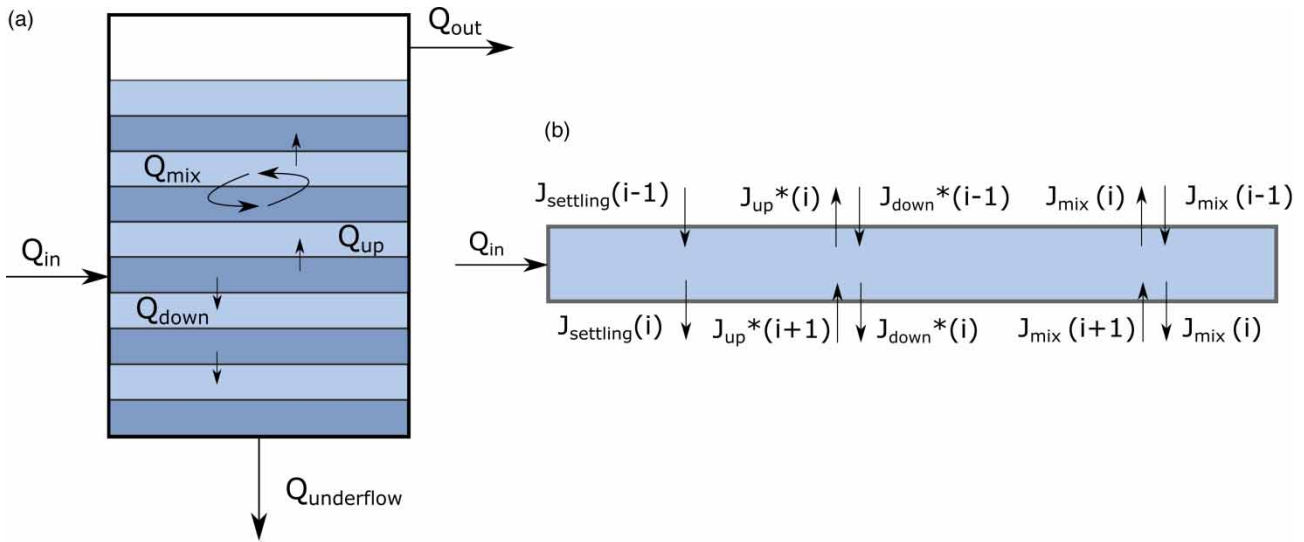


Figure 3 | Diagram of the hydraulic model. Representation of the interaction of the different variables comprising the model considering (a) the Q_{mix} and (b) the pollutant flux on the feed layer, including the flux due to mixing (U_{mix}). The '*' indicates the optional presence above or below the feed layer.

where Q_{mix} is the mixing flow between layers due to the vortex forces (m^3/d), and A is the surface of the grit chamber (m^2).

RESULTS AND DISCUSSION

Characterization of PSVD

First, at the inlet of the grit chamber, the settling characteristics were determined using 16 samples ranging in TSS

between 110 and 330 mg/L collected under different flow conditions during dry weather conditions. As mentioned in Plana *et al.* (2019), when analysing the ensemble of the 16 measured PSVD curves, it was observed that their location in the ViCAs curves shows a relationship with the inlet TSS concentration of the sample, i.e. at a higher concentration, the PSVD curve is located in the lower region, as indicated in Figure 4 (this relation was also found in the studies of Marujouls *et al.* 2011; Bachis *et al.* 2015). This variation is explained by the fact that, at higher flows, more particles are transported into the WRRF (higher TSS), and

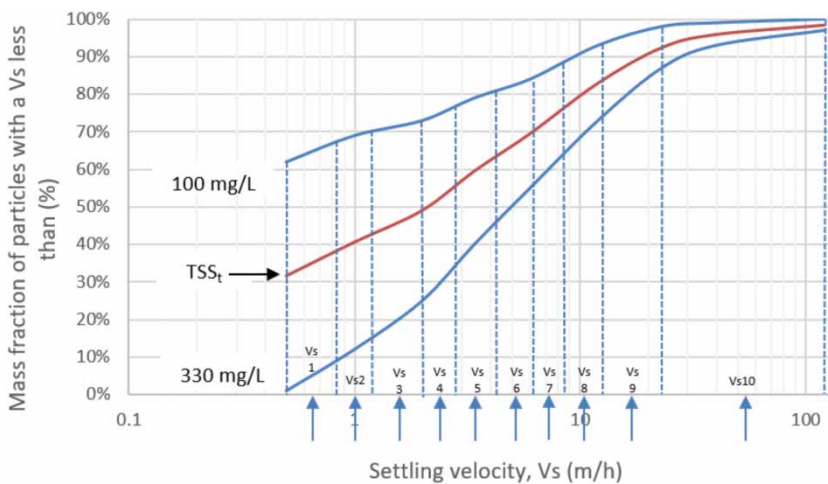


Figure 4 | Inlet PSVD settling velocity class boundaries for a particle class fractionation into ten classes. The arrows indicate the settling velocity that characterizes each class, calculated as the geometrical mean of the boundaries of each class. The blue curves are the PSVD curves limits determined experimentally: the lower boundary is the PSVD of the highest TSS concentration (330 mg/L), and the upper boundary is the PSVD of the lowest TSS concentration (100 mg/L). The red curve represents the PSVD for a given TSS concentration at a time t (TSS_t). Please refer to the online version of the paper to see this figure in colour: <http://dx.doi.org/10.2166/wst.2020.108>.

that generally these particles are characterized by higher settling velocities because these higher flows have more energy, allowing the resuspending of these faster settling particles.

Furthermore, the minimum settling velocity measured with the ViCAs tests was 2 m/h. To better represent more particle classes, the ViCAs curves were extended down to 0.5 m/h, as depicted in Figure 4. Each boundary was enlarged following the equation:

$$F_{v_s} = b \times \ln(v_s) + a \quad (4)$$

where $F_{v_s}(-)$ is the estimated fraction for a given settling velocity, v_s is the settling velocity (m/h), and a and b are coefficients of the logarithmic regression. First, the a and b coefficients were adjusted to the experimental curves. Then, the two equations for each boundary were used to estimate the settling velocities down to 0.5 m/h.

The PSVD curves obtained with the 2 m ViCAs column were described by ten particle classes. This number of classes was selected because it was concluded in the study by Tik (2020) that the PSVD model performs best without excessive calculation time. Each particle class is characterized by a mean settling velocity (see Figure 4). The boundaries of the ten classes were chosen considering ten equal fractions of the average PSVD curve. Then, from the established boundaries, the geometrical means of the boundaries were determined and set as the class settling velocities. For this study, the particle classes with their settling velocities are presented in Table 1.

Since the TSS concentration at the inlet of the grit chamber is varying continuously, the PSVD curve

Table 1 | Particle classes characterized by their settling velocity determined for the studied vortex grit chamber

Particle class	Settling velocity (m/h)
Class 1	0.67
Class 2	1.04
Class 3	1.63
Class 4	2.35
Class 5	3.44
Class 6	5.21
Class 7	7.50
Class 8	10.63
Class 9	17.71
Class 10	71.46

corresponding to a given TSS concentration is estimated at each time step. To estimate the PSVD, given a TSS concentration between the boundaries (i.e. between 100 and 330 mg/L), the cumulative fraction for each particle class is determined by linear interpolation (Tik 2020).

In case the inlet TSS concentration is outside the boundaries, the PSVD curve is determined by exponentially extrapolating the cumulative fraction for each particle class (Equations (5) and (7)). For example, when the TSS concentration is below the lowest concentration boundary (i.e. 100 mg/L for this case study), the cumulative fractions for each particle class to obtain the PSVD curve are calculated following the equation:

$$F_{v_s}(TSS) = F_{v_s}^{\max} + (F_{v_s}^{\text{low}} - F_{v_s}^{\max}) \times e^{-k_{\text{low}}(TSS_{\text{low}} - TSS)} \quad (5)$$

where $F_{v_s}(TSS)(-)$ is the cumulative fraction for each particle class given a TSS (mg/L), $F_{v_s}^{\max}(-)$ is the maximum cumulative fraction for each particle class, the $F_{v_s}^{\text{low}}(-)$ is the cumulative fraction for the lowest TSS concentration boundary for each particle class, k_{low} (L/mg) is the constant defining how 'fast' the curve approaches $F_{v_s}^{\max}$, TSS_{low} is the lowest concentration boundary observed from the ViCAs tests (mg/L) and TSS is the concentration under study (mg/L).

Considering that the $F_{v_s}^{\max}$ is 1 and $TSS_{\text{low}} = 100$ mg/L in this case study, Equation (5) can be simplified to:

$$F_{v_s}(TSS) = 1 + (F_{v_s}^{\text{low}} - 1) \times e^{-k_{\text{low}}(100 - TSS)} \quad (6)$$

To estimate k_{low} , it was considered that the fraction limit of 1 should be reached at 1/3 of the TSS limits (i.e. TSS_{min}). Thus, $k_{\text{low}} = 1/(100 - TSS)$. For $TSS_{\text{min}} = 0$ mg/L, k_{low} becomes 1/100 L/mg.

In contrast, when the TSS concentration is above the highest concentration observed within the ViCAs tests (i.e. 330 mg/L for this case study), the cumulative fraction for each particle class above this limit TSS concentration is estimated with the equation:

$$F_{v_s}(TSS) = F_{v_s}^{\min} + (F_{v_s}^{\text{high}} - F_{v_s}^{\min}) \times e^{-k_{\text{high}}(TSS - TSS_{\text{high}})} \quad (7)$$

where $F_{v_s}^{\min}(-)$ is the minimum cumulative fraction for each particle class, $F_{v_s}^{\text{high}}(-)$ is the cumulative fraction of the highest TSS concentration boundary for each particle class, k_{high} (L/mg) is the constant defining how 'fast' the curve approaches $F_{v_s}^{\min}$ and TSS_{high} is the highest concentration boundary observed from the ViCAs tests (mg/L).

For higher concentrations, considering $F_{v_s}^{\min} = 0$ and $TSS_{\text{high}} = 330 \text{ mg/L}$, Equation (7) becomes:

$$F_{v_s}(TSS) = F_{v_s}^{\text{high}} \times e^{-k_{\text{high}}(TSS-330)} \quad (8)$$

Similar to the case of TSS concentrations lower than 100 mg/L, for TSS concentrations higher than 330 mg/L, k_{high} can be estimated considering that the fraction limit is reached at 1/3 of the TSS limits (i.e. TSS_{max}). Then, $k_{\text{high}} = 1/(TSS-330) \text{ L/mg}$. If, for security, a large TSS concentration is set as a TSS limit (for example $TSS_{\text{max}} = 10,000 \text{ mg/L}$), k_{high} would become 1/9,670 L/mg.

The extrapolated curves considering minimum and maximum TSS concentrations as 0 and 10,000 mg/L, respectively, are presented in Figure 5 for this case study. The PSVD curves for modelling can of course be estimated for an even wider range of TSS concentrations at the inlet.

Inlet and outlet TSS dynamics

Monitoring the inlet and the outlet of the grit chamber, the solids dynamics were tracked. Figure 6 shows an example of typical dry weather flow and Figure 7 shows how the TSS concentrations vary at the inlet and the outlet of the grit chamber

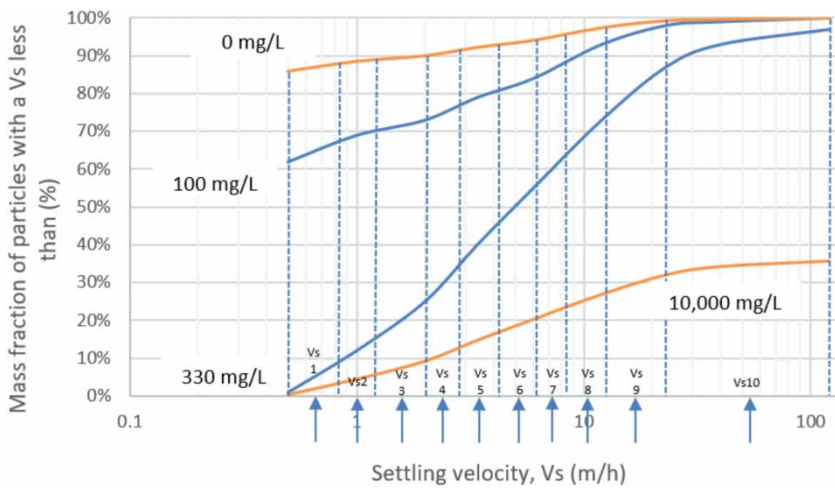


Figure 5 | Inlet PSVD settling velocity class boundaries (in blue) and extrapolated boundaries (in orange) for a particle class fractionation into ten classes. The arrows indicate the settling velocity that characterizes each class, calculated as the geometrical mean of the boundaries of each class. Please refer to the online version of the paper to see this figure in colour: <http://dx.doi.org/10.2166/wst.2020.108>.

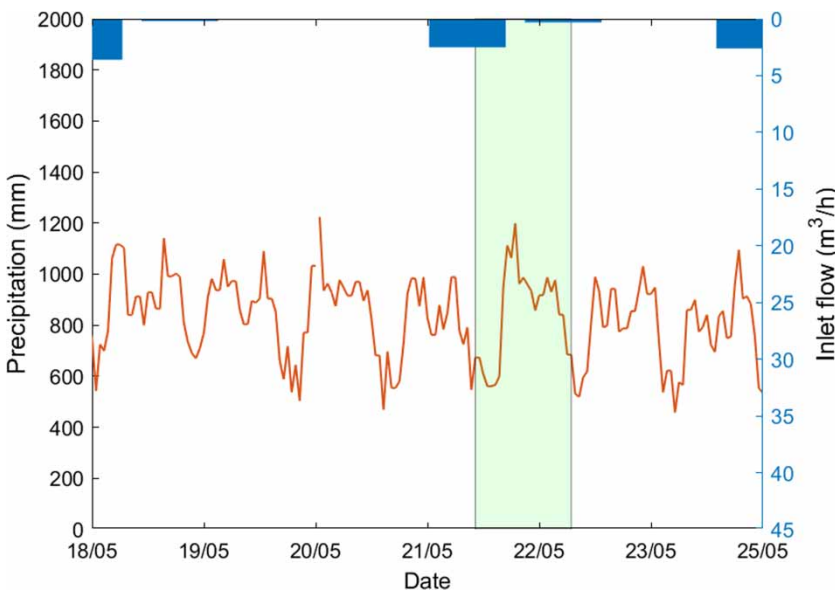


Figure 6 | Inlet hourly flow and precipitation from May 18 to May 26, 2017. The green square indicates the period of the calibration data set. Please refer to the online version of the paper to see this figure in colour: <http://dx.doi.org/10.2166/wst.2020.108>.

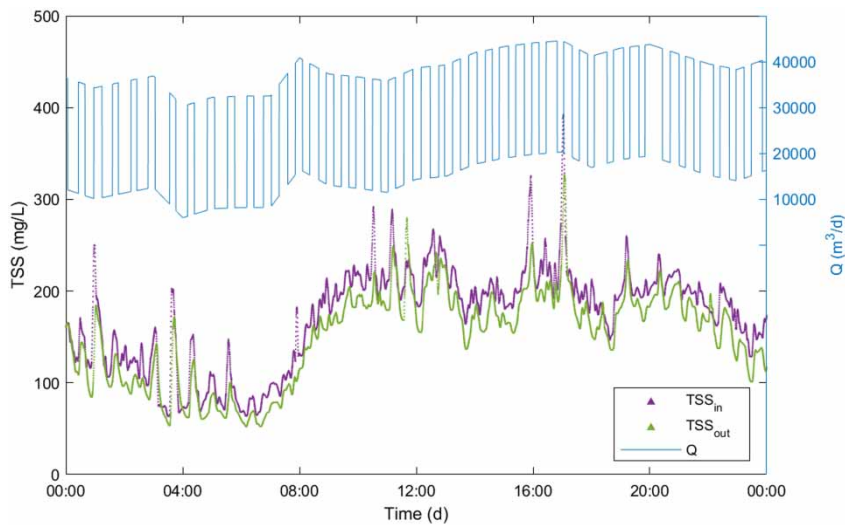


Figure 7 | On-line TSS measurements for calibration at the inlet and outlet of the studied system, together with the simulated inlet flow.

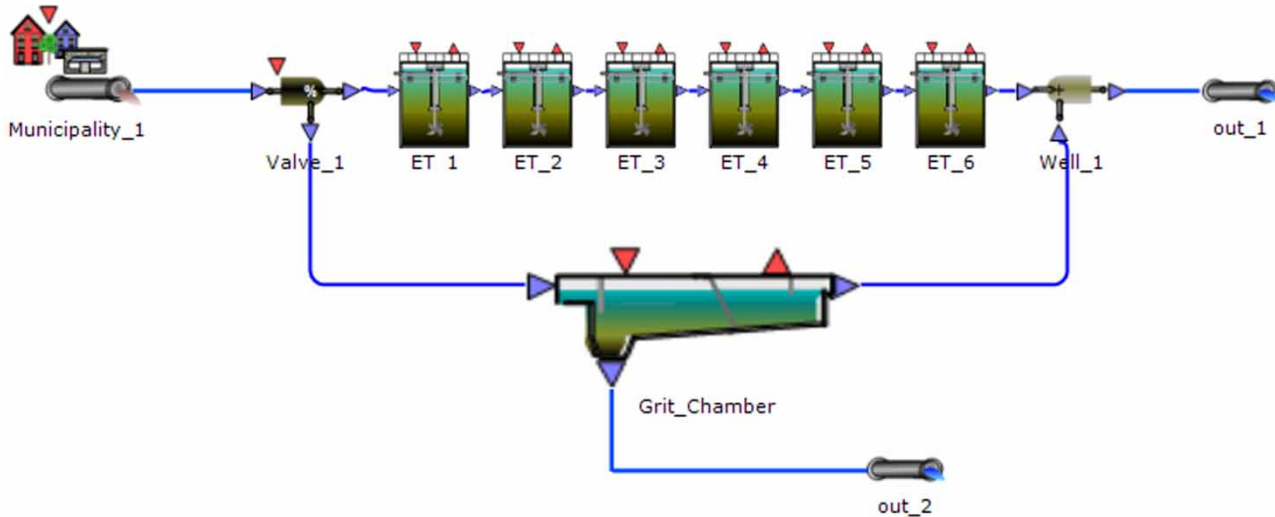


Figure 8 | Scheme of the hydraulic model for the vortex grit chamber. One-third of the flow is short-circuited to the outlet through the six tanks in series and the settler section is presented by the settler icon.

under dry weather flow conditions. Remarkably, the sudden inlet flow variations induced by a large on/off pumping station have a direct impact on the TSS concentrations, both at the inlet and outlet. They also affect the retention time of the grit chamber (varying between 1 and 4 min, in this case study) and, thus, the removal efficiency. Despite the fact that the flow and the pumping sequences are important for the grit chamber performance due to the low retention time, only hourly flowrate data were available from the facility. Hence, the actual high-frequency flowrate data ($\Delta t = 10$ sec) used to model the grit chamber were obtained with a physical model, only considering the data available (i.e. hourly inlet flow, high-frequency on-line temperature data, two days of

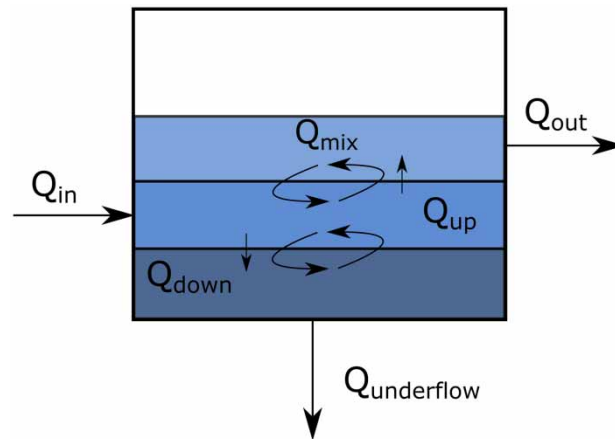


Figure 9 | Three-layer PSVD model with the flow behaviour into the vortex grit chamber.

detailed inlet flow at $\Delta t = 10$ sec, and physical characteristics of the pump station) (Plana 2020).

Hydraulic model

From the two tracer tests, a 1-D hydraulic model of the grit chamber was built in WEST. The tracer dynamics show that

part of the flow short-circuited very quickly through the grit chamber. This fraction of the flow was estimated by fitting the 1-D hydraulic model to the tracer data and the optimal was found to be at a fraction of one-third. The other two-thirds were considered passing through the settler section (see Figure 8).

To represent the short-circuited flow, several configurations were tested in terms of number of tanks in

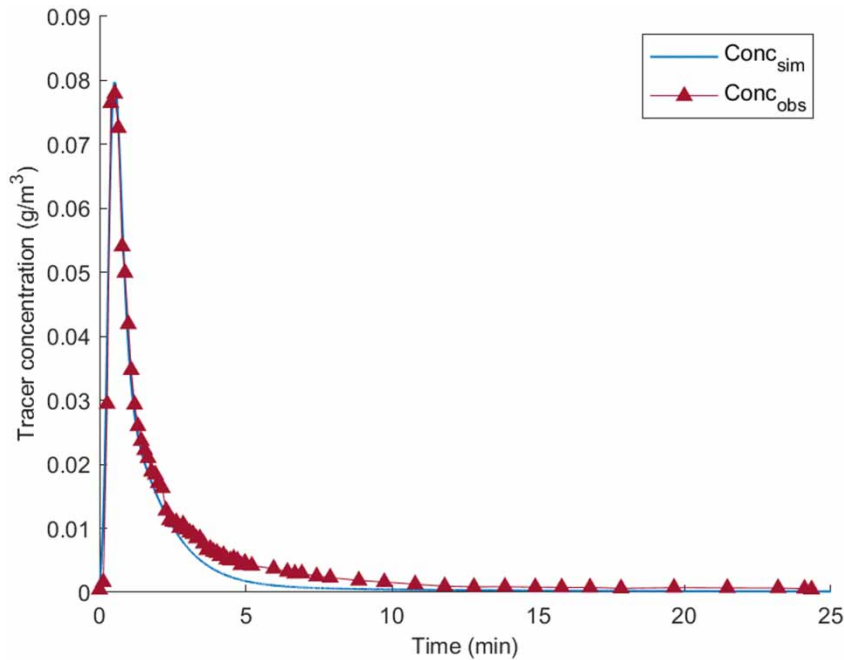


Figure 10 | Simulated and observed results of the second test.

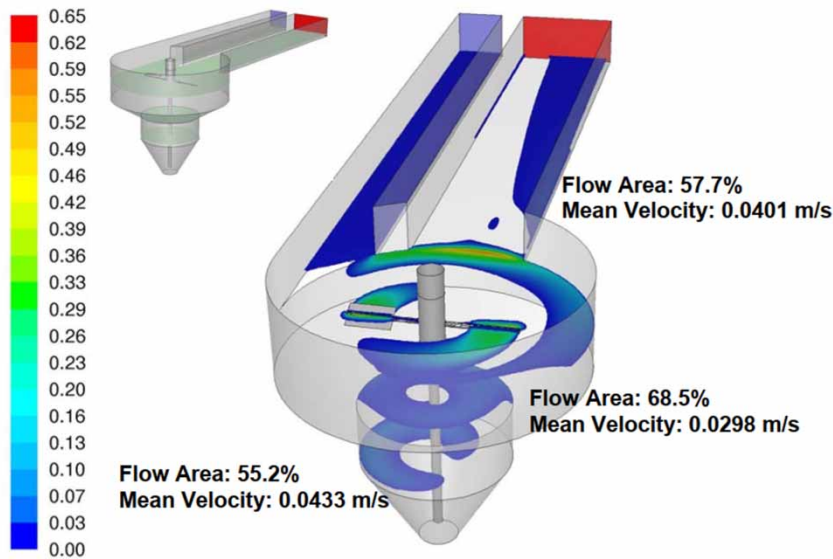


Figure 11 | Particle velocity tracked of three horizontal CFD model sections of a vortex grit chamber (Couture *et al.* 2009).

series and tank volume. The best fit for both tracer tests was six tanks in series of 0.3 m^3 each, as depicted in Figure 8. This volume corresponds to a layer of 13 cm at the top of the occupied volume of the grit chamber, which corresponds to the water height at the inlet channel. In addition, the tracer test suggested three vertical layers (two between inlet and outlet, and one sediment layer to the underflow) to represent the hydraulic behaviour of the settling tank part as presented in Figure 9. Given the occupied real volume of about 16 m^3 , knowing that the surface of the grit chamber is 13.85 m^2 , the volume per layer coincides with the volume of the lower part of the grit chamber. The height of the settler was calculated as 1.16 m. Thus, the height of each layer is 0.39 m. The depicted arrows

in Figure 9 represent the flow behaviour in the settler. As mentioned previously, the Q_{mix} represent the mixing flow induced by the vortex forces inside the real grit chamber.

As a result of the adjustments presented above to represent the hydraulics of the grit chamber, experimental and simulated results for the second tracer test are compared (see Figure 10). A good fit of the hydraulic model can be noticed with a root mean squared error (RMSE) of 0.0017 mg/L of tracer.

Importantly, this hydraulic model agrees with the behaviour observed in CFD studies performed by the industrial partner, Veolia Water Technologies Canada, on a vortex grit chamber with the same configuration as the studied unit (see Figure 11) (Couture *et al.* 2009): there is a part of

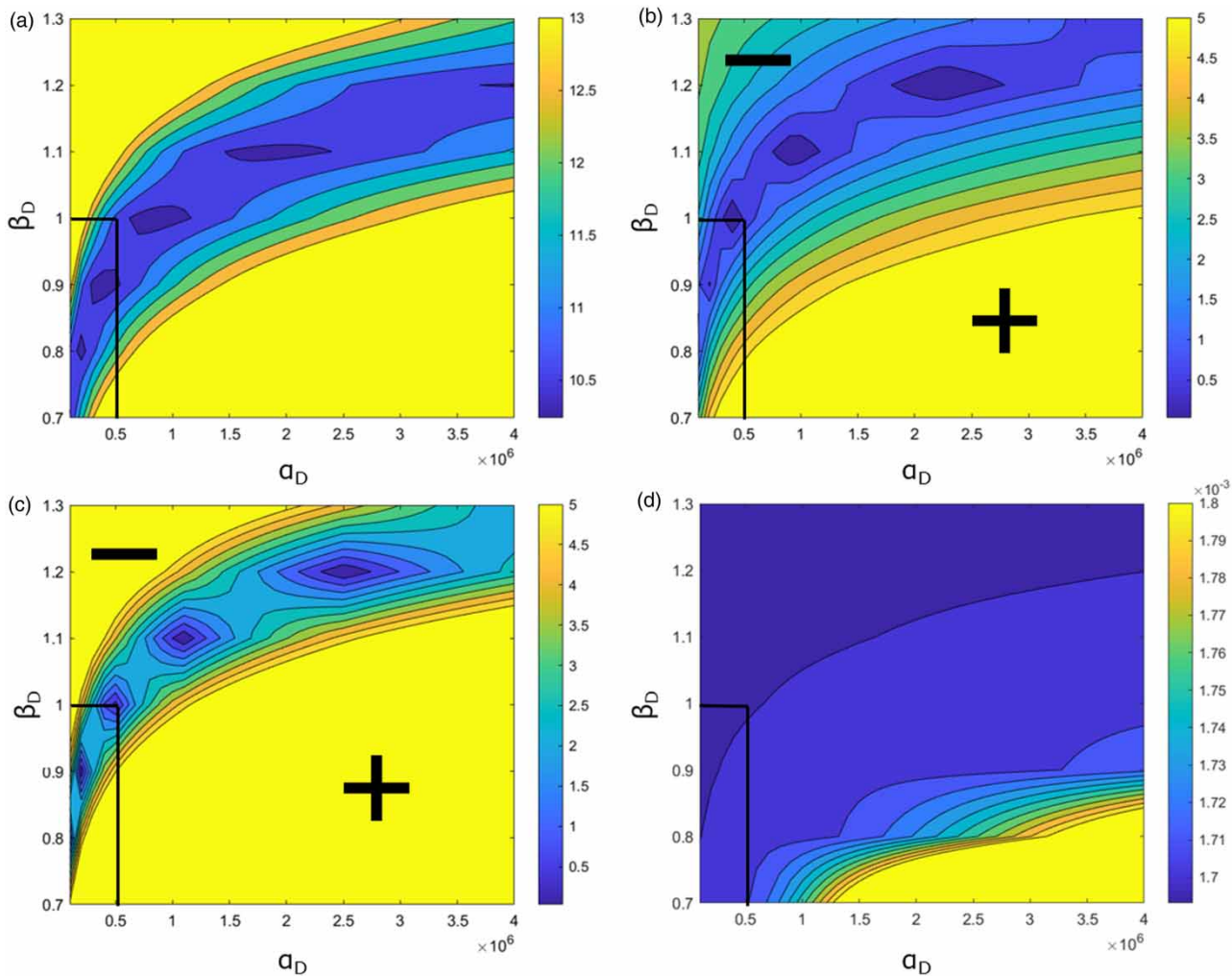


Figure 12 | Calculation results for the vortex model calibration: (a) RMSE results of the PSVD model for a range of α_D and β_D values, (b) absolute value of the difference between the observed and simulated percentage removal, (c) absolute values of the bias, and (d) RMSE results of the hydraulic model. The + and - symbols represent the positive and negative zone values. The crossing black lines indicate the set of parameters selected.

the flow short-circuiting the grit chamber, and another part passing through the settling section

Calibration of PSVD model

The removal performance of the ten-particle-classes model can now be calibrated through comparing the proposed model with a one-day on-line TSS data set. The data set used for model calibration was obtained under dry weather conditions (see Figures 6 and 7).

First, the physical model parameters of the hydraulic model (i.e. surface area and height of the grit chamber) were set to the physical characteristics and operation conditions. Despite the fact that the grit removal is performed at discrete times from the bottom of the grit chamber, the underflow was assumed constant and at a low flowrate so that it does not affect the grit chamber hydraulics. This assumption could be made because the height of the particles accumulated at the bottom of the grit chamber does not exceed 80% of the height of the lower part of the studied vortex grit chamber. The volume of that part coincides with the volume of the lower layer of the settler, which is considered only as a settling zone.

Not calibrating any model parameter further and only using the ViCAs-derived settling velocity parameters (see previous section on PSVD fractionation), a promising fit to the data was obtained, albeit with a slightly overestimated removal performance (results not shown). To

improve the fit, the backmixing parameters were considered a good handle to obtain a better fit to the observed removal efficiency. The mixing flow between the layers, leading to a resuspension of particles, was therefore augmented.

The removal efficiency of the grit chamber obviously varies with flow conditions: at low flow, due to the higher retention time, the removal is higher and particles with low settling velocities can be removed to some extent. Conversely, in high flow conditions, the retention time is reduced, leading to a lower removal, and most of the particles that are removed are the ones that settle fast.

However, when a fixed Q_{mix} was used, it was found that the removal efficiency was overpredicted in low flow conditions and underpredicted in high flow. To accommodate for this, the Q_{mix} was made dependent on the inflow. In fact, backmixing, or dispersion, is higher in low flow conditions ('there is more time for dispersion'), as for instance, expressed in the models of Chambers & Jones (1988) and Gujer (2008). A turbulent dispersion mixing flow (Q_{mix}), inversely proportional to the inlet flow (Q_{in}), was proposed and its parameters estimated from Equation (9):

$$Q_{\text{mix}} = \frac{\alpha_D}{Q_{\text{in}}^{\beta_D}} \quad (9)$$

The parameters related to this mixing flow (dispersion factor, α_D ($(\text{m}^3/\text{d})^{\beta_D+1}$) and mixing behaviour, β_D (-))

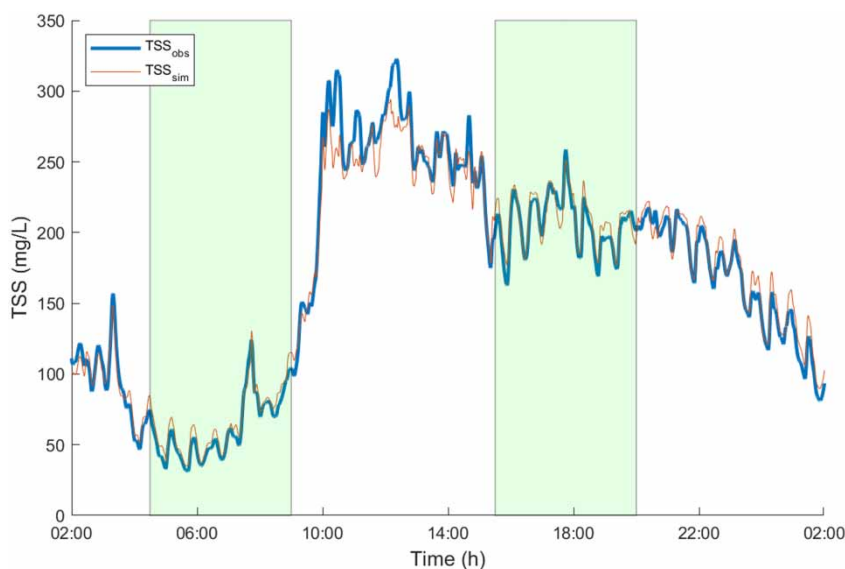


Figure 13 | Observed and simulated results at the outlet of the grit chamber for the calibration test under dry weather conditions: during the low flow period (left patch) with high backmixing conditions and during the high flow period (right patch) with low backmixing conditions.

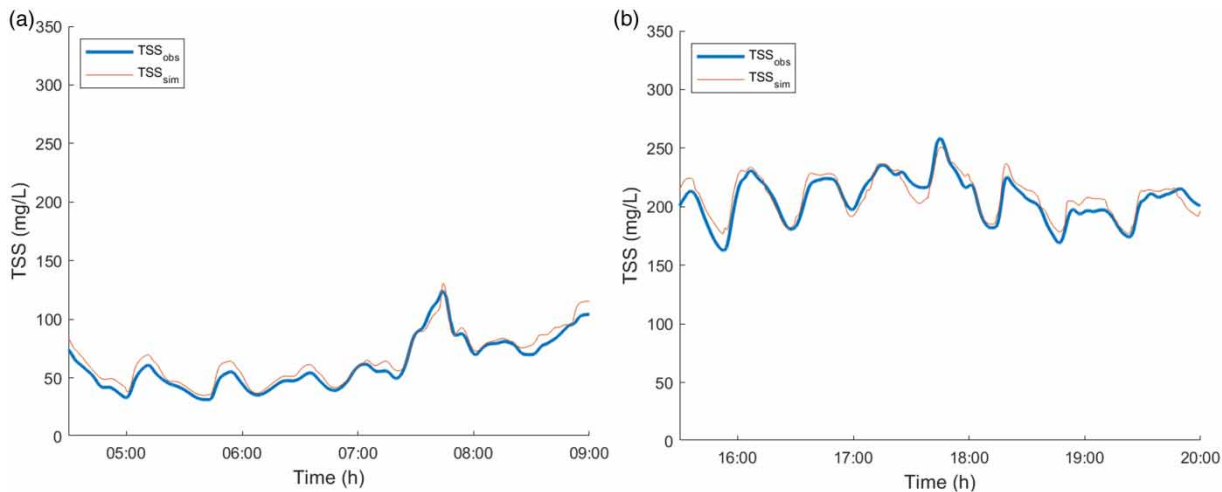


Figure 14 | Zoom of the observed and simulated TSS concentrations at (a) low flow and (b) high flow.

between the model layers, were determined by fitting the model to the selected data set for the PSVD-model calibration. The goodness-of-fit of the model was statistically estimated with the RMSE, the bias and the difference in the percentage removal criterion. The results of the calculations performed to select the best set of parameters are presented in Figure 12.

The results of the calibrated model show a good approximation of the outlet TSS and their dynamics (see Figures 13 and 14 for detailed results at low and high flows). The simulated overall removal efficiency of 8.7% was similar to the measured removal of 8.5%. The estimated RMSE was 10.9 mg/L, which represents 6% of the average TSS concentration and is of the same order of magnitude as the measurement errors of the TSS sensors. Finally, the estimated bias was 0.31 mg/L, which is very close to 0. Comparing these results with the ones obtained with a constant Q_{mix} (for the best fit, the RMSE was 15.9 mg/L, representing 9.5% of the average TSS concentration, the bias was 5.9 mg/L, and the simulated overall removal efficiency was 1.3%), the better performance of the model including dynamic Q_{mix} is stated to be relevant.

In Table 2, the overall impact of the inlet flow on the percentage removal can be observed for each particle class during the calibration test. A key feature of the model is, of course, that it is capable of capturing the more efficient removal of the particles with higher settling velocities (i.e. classes 8–10). This behaviour is also noticed when comparing the overall PSVD curves from the inlet, outlet and underflow (see Figure 15). It can be observed that the particles at the outlet are settling slower than at

Table 2 | Percentage removal of each particle class characterized by their settling velocity for the calibration test

Particle class	Settling velocity (m/h)	Concentration (mg/L)	% mass	% removal
Class 1	0.67	67.6	38%	9%
Class 2	1.04	9.6	5%	8%
Class 3	1.63	14.5	8%	1%
Class 4	2.35	11.1	6%	2%
Class 5	3.44	17.1	10%	3%
Class 6	5.21	16.2	9%	5%
Class 7	7.50	12.5	7%	10%
Class 8	10.63	9.5	5%	15%
Class 9	17.71	11.1	6%	23%
Class 10	71.46	10.8	6%	57%
<i>Total</i>		<i>180.1</i>		<i>8.5%</i>

the inlet. Also, the particles at the underflow are settling much faster than those at the inlet. Hence, the percentage of fast-settling particles is higher at the underflow, which means that they are mostly removed by the grit chamber.

Following the model calibration, an analysis of the residuals was also performed to evaluate whether the model provides a good description of the data (Dochain & Vanrolleghem 2001; Box et al. 2005). The difference between the time series of observed and simulated data shows that there is no tendency of the particles' removal over time. The residuals have also been plotted versus two variables of interest, i.e. the TSS concentration and the inlet flow.

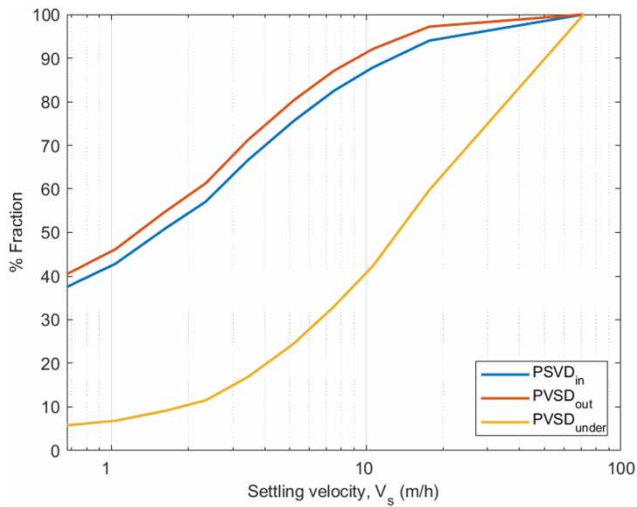


Figure 15 | Fractions estimated for each particle class from the one-day data set for the inlet, outlet and underflow.

For example, the residuals versus TSS concentration plot suggests a certain trend: at low TSS concentrations, generally the particles' removal is underestimated, while at higher TSS concentrations, the particles' removal seems to be mostly overestimated. Regarding the residuals versus inlet flow plot, no clear tendency could be detected. The plots obtained from the residuals analysis are presented in Figure 16.

Validation of the PSVD model

The model was validated by testing it under quite different conditions, with two other data sets collected under different weather conditions: first, during winter-time (see Figure 17) and, then, under wet weather conditions during summer-time (see Figure 18).

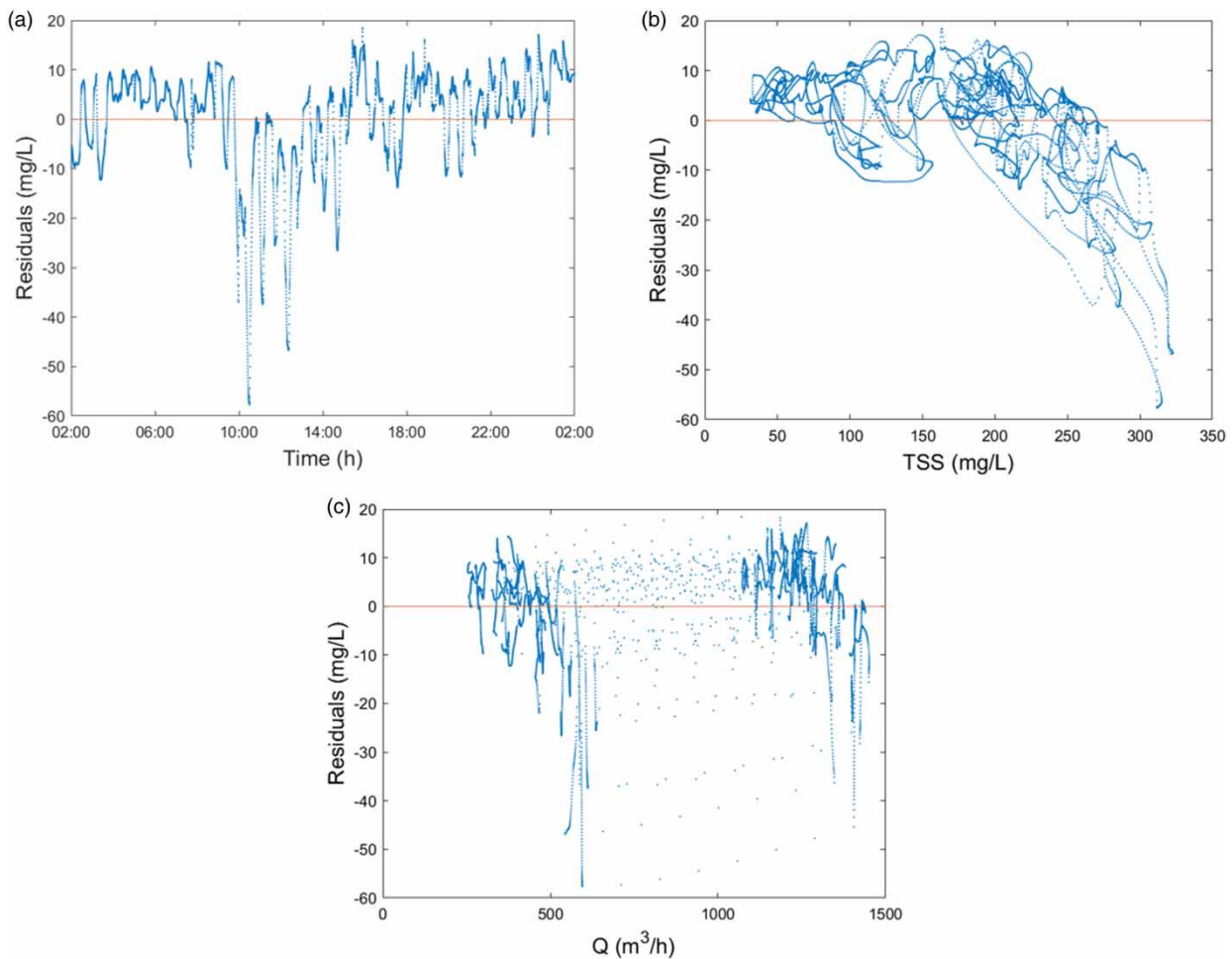


Figure 16 | Analysis of the residuals of the calibration test for the vortex grit chamber: (a) residuals in time sequence, (b) residuals versus TSS concentration, and (c) residuals versus inlet flow.

The validation of the winter-time data set was considered to be conducted under dry weather conditions since the snowfall did not affect the inflow, as depicted in Figure 17. The TSS data set used is presented in Figure 19 with the simulated inlet flow at high frequency.

The results obtained confirmed the good performance of the model, reproducing the outlet TSS concentrations

and their dynamics (see Figure 20). This time, the percentage removal simulated was 7%, which is slightly different than the 11% observed, although both are of the same order of magnitude. The RMSE was 16.8 mg/L, which represents 10% of the average TSS concentration along the data set. The bias estimated for the validation equals 10 mg/L. Thus, the bias indicates that the model is globally underpredicting the particle removal efficiency since the

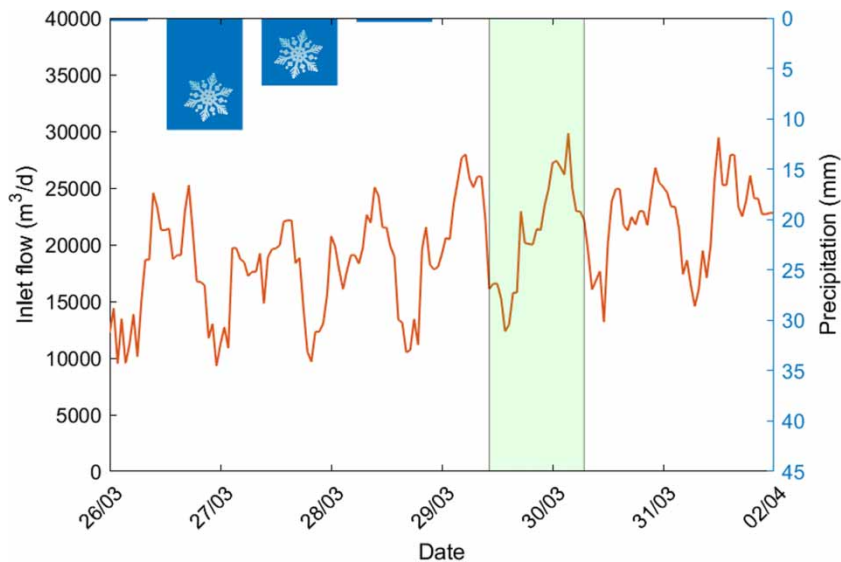


Figure 17 | Inlet hourly flow and precipitation from March 26 to April 2, 2017. The green square indicates the period of the validation data set during winter-time. Please refer to the online version of the paper to see this figure in colour: <http://dx.doi.org/10.2166/wst.2020.108>.

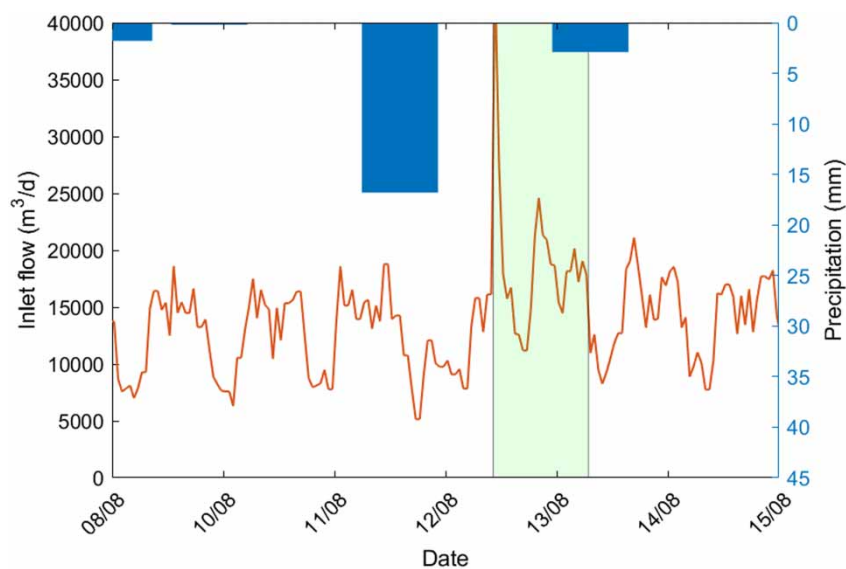


Figure 18 | Inlet hourly flow and precipitation from August 9 to August 15, 2017. The green square indicates the period of the validation data set under wet weather conditions. Please refer to the online version of the paper to see this figure in colour: <http://dx.doi.org/10.2166/wst.2020.108>.

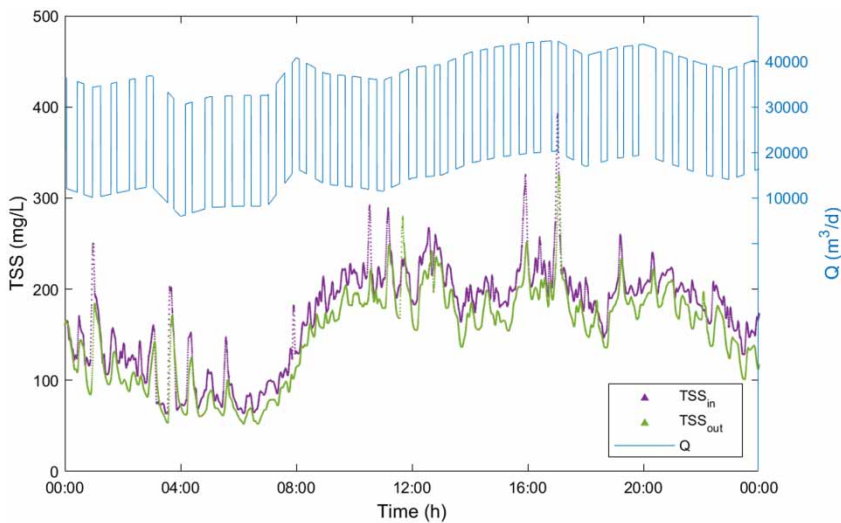


Figure 19 | On-line TSS measurements for model validation under dry weather winter conditions at the inlet and outlet of the grit chamber with the simulated inlet flow.

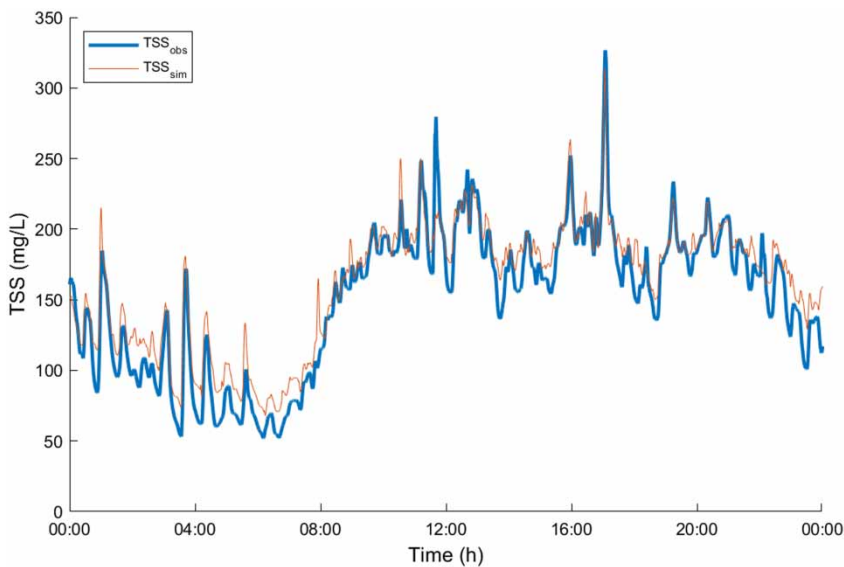


Figure 20 | Observed and simulated results in dry weather winter conditions at the outlet of the grit chamber for the validation test.

estimated TSS is overall 10 mg/L above the observed TSS. By comparing the obtained validation RMSE with the calibration RMSE, the Janus coefficient could be estimated, and it was equal to 1.5 (Sin *et al.* 2008; Rieger *et al.* 2013). Thus, this validation was successful (Janus coefficient <2).

Regarding the percentage removal of each fraction, results similar to the calibration results were observed (Table 3). Again, the percentage removal is higher for fractions with a higher settling velocity (i.e. classes 8–10).

To complete the evaluation of the first validation test, an analysis of the residuals was again performed. In Figure 21, a bias is observed in the three plots of the residuals versus time, TSS concentration and inlet flow similar to Figure 20. This may be explained by the water temperature being lower during winter, leading to a higher water viscosity. With the increase of viscosity, the settling velocity of the particles decreases leading to lower particle removal. Despite the bias (10 mg/L), the residuals are distributed randomly for the three variables.

Table 3 | % removal of each particle class characterized by their settling velocity for the validation test under dry weather conditions

Particle class	Settling velocity (m/h)	Concentration (mg/L)	% mass	% removal
Class 1	0.67	79.7	47%	1%
Class 2	1.04	8.3	5%	2%
Class 3	1.63	12.6	7%	2%
Class 4	2.35	9.7	6%	3%
Class 5	3.44	14.9	9%	5%
Class 6	5.21	14.1	8%	7%
Class 7	7.50	10.8	6%	11%
Class 8	10.63	7.1	4%	15%
Class 9	17.71	7.5	4%	25%
Class 10	71.46	7.3	4%	58%
<i>Total</i>		<i>171.9</i>		<i>6.9%</i>

The second validation test was performed with data collected under wet weather conditions as mentioned above and shown in Figure 18. The high peak flowrate had an impact on the TSS concentrations at the inlet and at the outlet as depicted in Figure 22. Also in Figure 22, it can be noticed that the pump activations are longer at high flow than under dry weather conditions for the same time during the day.

The results obtained from the second validation confirmed the good performance of the model. The model was able to reproduce the outlet TSS concentrations and their dynamics, even under wet weather conditions (see Figure 23).

The percentage removal simulated was 10%. Compared with the 13% observed, the simulated removal is slightly lower, but the order of magnitude is again the same. The

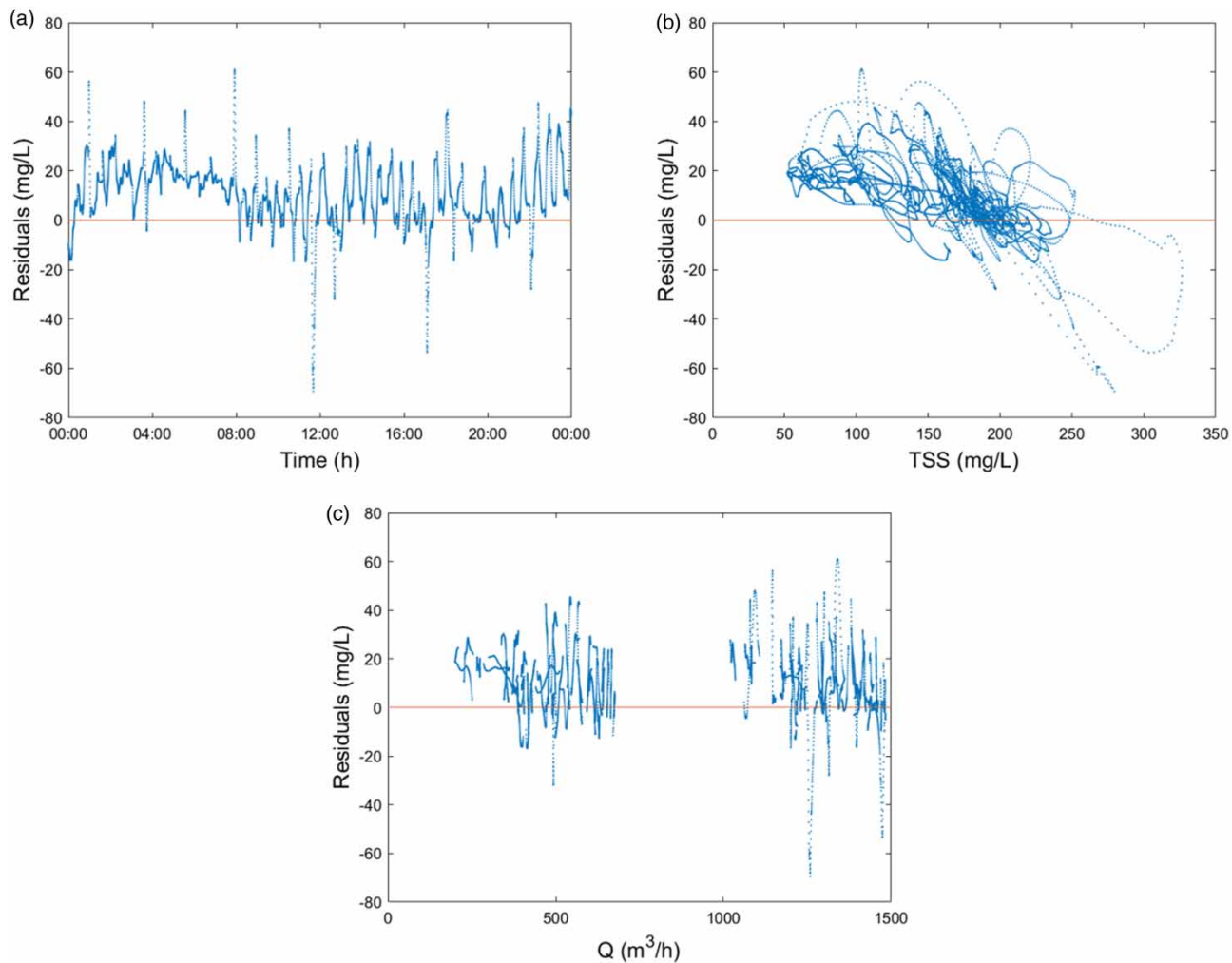


Figure 21 | Analysis of the residuals of the validation test under dry weather winter-time conditions for the vortex grit chamber: (a) residuals in time sequence, (b) residuals versus TSS concentration, and (c) residuals versus inlet flow.

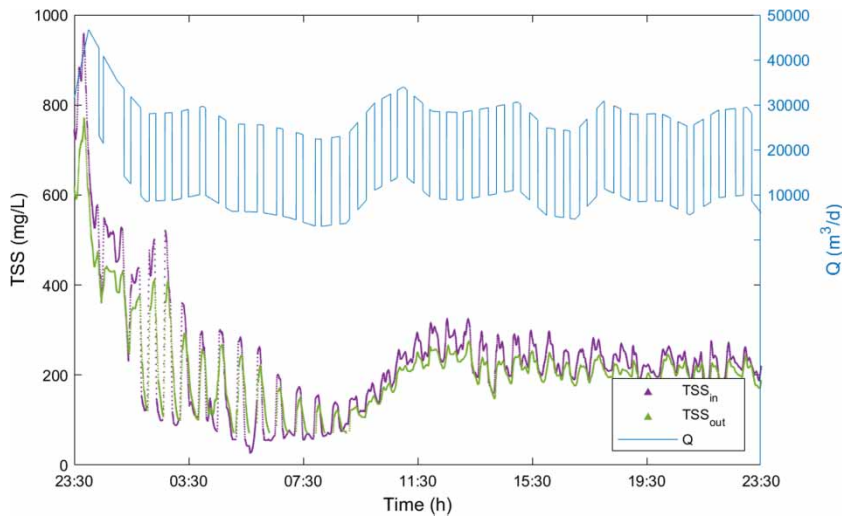


Figure 22 | On-line TSS measurements for model validation under wet weather summer conditions at the inlet and outlet of the grit chamber with the simulated inlet flow.

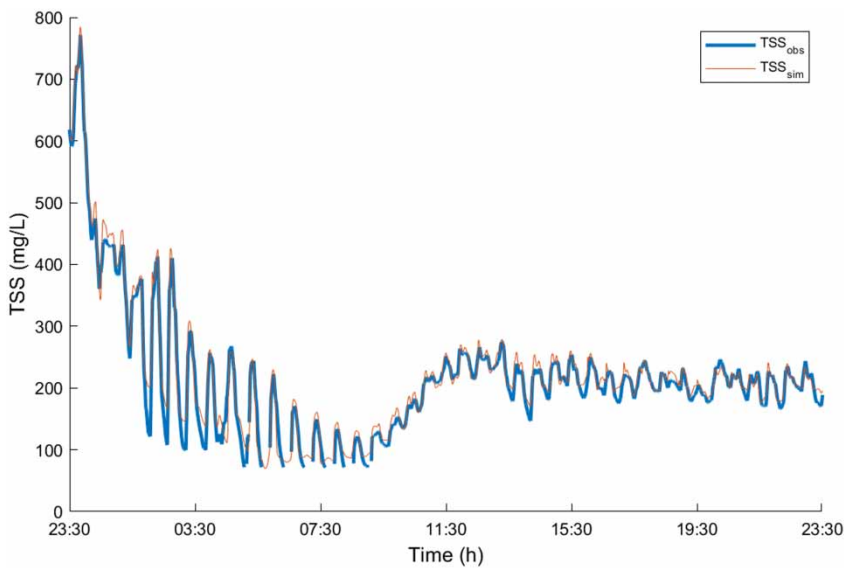


Figure 23 | Observed and simulated TSS data under wet weather summer conditions at the outlet of the grit chamber for the validation test.

estimated RMSE was 16.7 mg/L. Despite the similar RMSE on both validation tests, in this case, it only represents 7% of the average TSS concentration given the higher inlet concentration under this rain event. The bias estimated for this validation is 6 mg/L. Again, the model is slightly underestimating the particles' removal. However, the obtained bias is lower than the bias for the first validation. Finally, comparing the RMSE for the calibration and this validation, the Janus coefficient is also 1.5. Thus, the second validation test was also successful (Janus coefficient <2).

Similar to the results presented above, the percentage removals of each particle class show that fast-settling particles are removed better (see Table 4). In contrast to the previous data sets under dry weather conditions, the percentage of fast-settling particles is higher under wet weather conditions due to the high flow that is able to resuspend particles accumulated in the sewer system.

Furthermore, as for the calibration test and the first validation test, to better understand the simulated results, the residuals were also studied for this validation test. In contrast to the previous validation test, no bias was

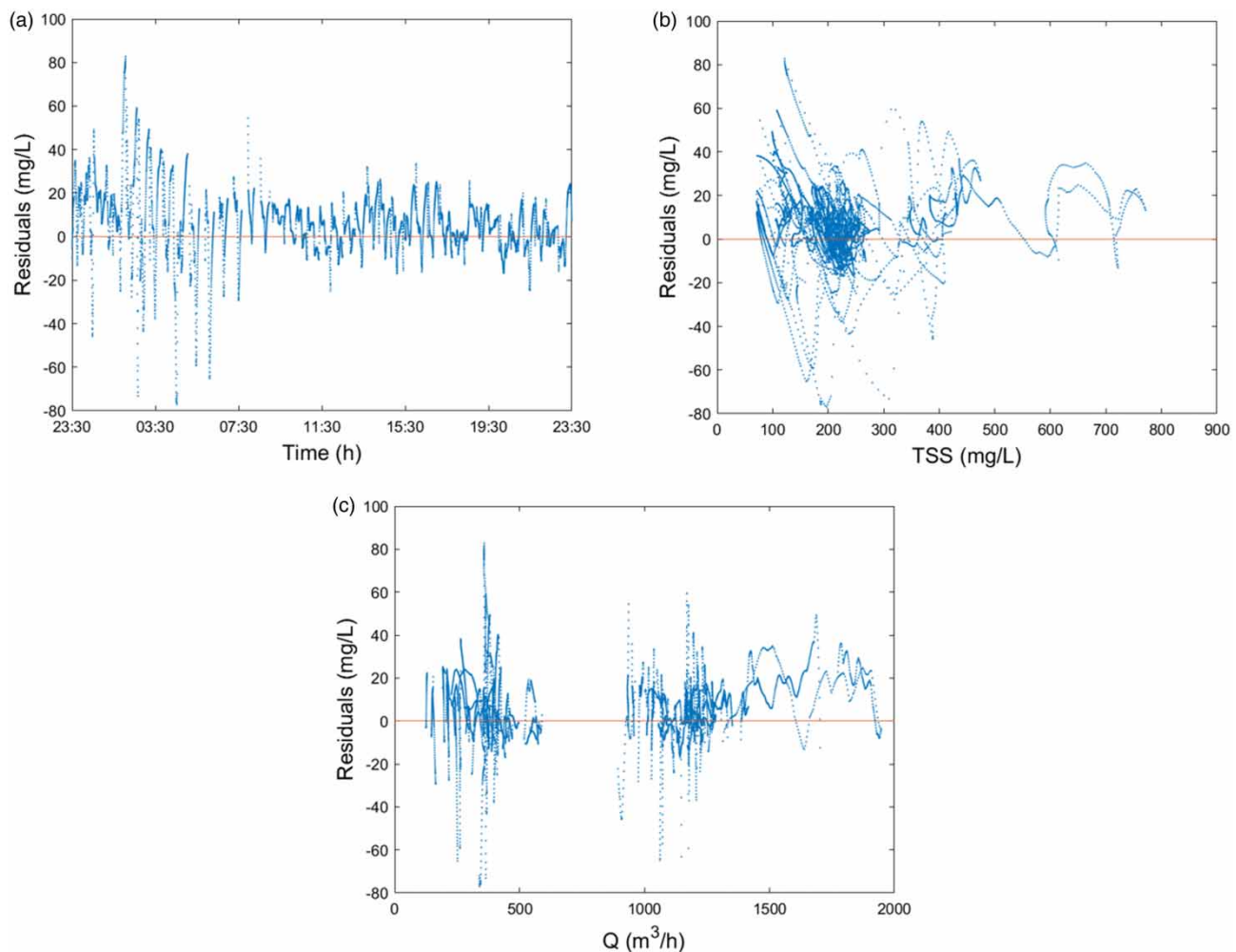
Table 4 | Percentage removal of each particle class characterized by their settling velocity for the validation test under wet weather conditions

Particle class	Settling velocity (m/h)	Concentration (mg/L)	% mass	% removal
Class 1	0.67	67.1	28%	1%
Class 2	1.04	13.8	6%	1%
Class 3	1.63	20.9	9%	2%
Class 4	2.35	15.9	7%	2%
Class 5	3.44	24.6	10%	4%
Class 6	5.21	23.3	10%	6%
Class 7	7.50	18.0	8%	9%
Class 8	10.63	15.1	6%	12%
Class 9	17.71	18.7	8%	21%
Class 10	71.46	18.2	8%	56%
Total				9.2%

observed in the residuals (see Figure 24). The residuals in time sequence are distributed randomly around 0. However, the residuals show an underestimation of the TSS removal at higher TSS concentration and inlet flow.

CONCLUSIONS

Grit chambers need to be properly characterized in view of whole WRRF modelling, settling characteristics and hydraulic dynamics being the key characteristics. A new experimental characterization and modelling approach based on PSVD has been proposed and the new model was successfully calibrated and especially validated even under quite different operational conditions. Compared with the existing (static) grit chamber models, the proposed

**Figure 24** | Analysis of the residuals of the validation test under wet weather conditions for the vortex grit chamber: (a) residuals in time sequence, (b) residuals versus TSS concentration, and (c) residuals versus inlet flow.

dynamic model allows remarkably good dynamic predictions of effluent TSS and overall removal performance, including under wet weather conditions.

ACKNOWLEDGEMENTS

The authors thank the financial support by a Collaborative Research & Development grant of the Natural Sciences and Engineering Research Council (NSERC) and Veolia Water Technologies Canada. Peter Vanrolleghem holds the Canada Research Chair in Water Quality Modelling.

REFERENCES

- Alferes, J., Tik, S., Copp, J. & Vanrolleghem, P. A. 2013 *Advanced monitoring of water systems using in situ measurement stations: data validation and fault detection*. *Water Science and Technology* **68** (5), 1022–1030.
- Bachis, G., Maruéjols, T., Tik, S., Amerlinck, Y., Melcer, H., Nopens, I., Lessard, P. & Vanrolleghem, P. A. 2015 *Modelling and characterization of primary settlers in view of whole plant and resource recovery modelling*. *Water Science and Technology* **72** (12), 2251–2261.
- Box, G. E. P., Hunter, J. S. & Hunter, W. G. 2005 *Statistics for Experimenters: Design, Innovation, and Discovery*, 2nd edn. Wiley, Hoboken, NJ, USA.
- Chambers, B. & Jones, G. L. 1988 *Optimisation and uprating of activated sludge plants by efficient process design*. *Water Science and Technology* **20** (4–5), 121–132.
- Chebbo, G. & Gromaire, M.-C. 2009 *VICAS – an operating protocol to measure the distributions of suspended solid settling velocities within urban drainage samples*. *Journal of Environmental Engineering* **135** (9), 768–775.
- Couture, M., Steele, A., Bruneau, M., Gadbois, A. & Hohman, B. 2009 *Achieving greater efficiency for 360° rotational grit removal technology using empirical data and CFD analysis*. In: *Proceedings 82nd Water Environment Federation Technical Exhibition and Conference; WEFTEC2009*, 10–14 October, Orlando, FL, USA.
- Dochain, D. & Vanrolleghem, P. 2001 *Dynamical Modelling and Estimation in Wastewater Treatment Processes*. IWA Publishing, London, UK.
- Gujer, W. 2008 *Systems Analysis for Water Technology*. Springer, Berlin, Germany.
- Ledergerber, J. M., Maruéjols, T. & Vanrolleghem, P. A. 2019 *Optimal experimental design for calibration of a new sewer water quality model*. *Journal of Hydrology* **574**, 1020–1028.
- Maruéjols, T., Lessard, P., Wipliez, B., Pelletier, G. & Vanrolleghem, P. A. 2011 *Characterization of the potential impact of retention tank emptying on wastewater primary treatment: a new element for CSO management*. *Water Science and Technology* **64** (9), 1898–1905.
- Maruéjols, T., Vanrolleghem, P. A., Pelletier, G. & Lessard, P. 2012 *A phenomenological retention tank model using settling velocity distributions*. *Water Research* **46** (20), 6857–6867.
- Maruéjols, T., Lessard, P. & Vanrolleghem, P. A. 2015 *A particle settling velocity-based integrated model for dry and wet weather wastewater quality modeling*. In: *WEF Collection Systems Conference*, 19–22 April, Cincinnati, OH, USA.
- McNamara, B. F., Griffiths, J. & Book, D. 2009 *True grit. A grit removal efficiency investigation at five wastewater treatment plants*. In: *Proceedings 82nd Water Environment Federation Technical Exhibition and Conference; WEFTEC2009*, 10–14 October, Orlando, FL, USA.
- Plana, Q. 2020 *Characterization and Modelling of Grit Chambers Based on Particle Settling Velocity Distributions*. PhD thesis, Université Laval, Québec, QC, Canada.
- Plana, Q., Carpentier, J., Gagnon, L., Pauléat, A., Gadbois, A., Lessard, P. & Vanrolleghem, P. A. 2018 *Grit particle characterization: study of the settleability*. In: *Proceedings 91st Water Environment Federation Technical Exhibition and Conference; WEFTEC2018*, 29 September–3 October, New Orleans, LA, USA.
- Plana, Q., Pauléat, A., Gadbois, A., Lessard, P. & Vanrolleghem, P. A. 2019 *Characterizing the settleability of grit particles*. *Water Environment Research*. <https://doi.org/10.1002/wer.1268>.
- Qasim, S. R. 1999 *Wastewater Treatment Plants: Planning, Design, and Operation*, 2nd edn. Routledge, London, UK.
- Rieger, L., Gillot, S., Langergraber, G., Ohtsuki, T., Shaw, A., Takács, I. & Winkler, S. 2013 *Guidelines for Using Activated Sludge Models*. IWA Publishing, London, UK.
- Rife, J. C. & Botero, L. 2012 *Last of the neglected treatment processes: rewriting the manual of practice no. 8 section on grit removal*. In: *Proceedings 85th Water Environment Federation Technical Exhibition and Conference; WEFTEC2012*, 29 September–3 October, New Orleans, LA, USA.
- Sin, G., De Pauw, D. J. W., Weijers, S. & Vanrolleghem, P. A. 2008 *An efficient approach to automate the manual trial and error calibration of activated sludge models*. *Biotechnology and Bioengineering* **100** (3), 516–528.
- Tik, S. 2020 *Contrôle d'un système intégré d'assainissement urbain basé sur la qualité de l'eau – Vers des stratégies tolérantes aux fautes*. PhD thesis, Université Laval, Québec, QC, Canada (in French).
- Tik, S., Maruéjols, T., Bachis, G., Vallet, B., Lessard, P. & Vanrolleghem, P. A. 2014 *Using particle settling velocity distributions to better model the fate of stormwater TSS throughout the integrated urban wastewater system*. *Influents* **2014** (Winter), 48–52.
- Vallet, B., Muschalla, D., Lessard, P. & Vanrolleghem, P. A. 2014 *A new dynamic water quality model for stormwater basins as a tool for urban runoff management: concept and validation*. *Urban Water Journal* **11** (3), 211–220.
- WEF 2016 *Guidelines for Grit Sampling and Characterization*. Water Environment Federation, Alexandria, VA, USA.